The gate voltage shifts, ΔV_g, at a constant current density are plotted in Fig. 2. For RTO-67 (pure SiO_2), V_g is slightly shifted to the positive direction at the initial stage, and then

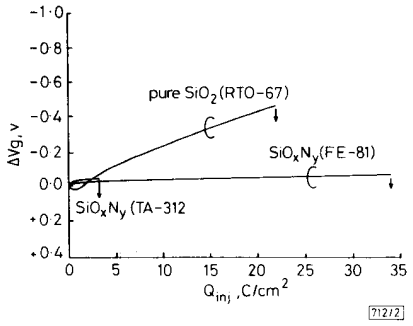

Fig. 2 *Gate voltage shift against injected charge*
RTO-67; TA-312; FE-81

increases almost linearly to the negative direction with increasing Q_{inj}. On the contrary, for TA-312 (SiO_xN_y) and FE-81 (SiO_xN_y), no positive V_g shifts are observed and the degrees of V_g shifts are much smaller than that in RTO-67. These findings indicate that the density of electron traps in RTO-67 is much larger than those in TA-312 and FE-81. It is considered that injected electrons are captured by the process: $O_3 \equiv Si^+ + e^- \rightarrow O_3 \equiv Si^*$. Therefore, it is quite possible that the formation of Si-N bonds plays an important role in reducing Si* defects. As is seen in Fig. 2, charge-to-breakdown, Q_{BD} increased in the order: TA-312 (SiO_xN_y), RTO-67 (SiO_2) and FE-81 (SiO_xN_y). This finding indicates that proper nitridation (FE-81) is also effective for improving the breakdown characteristics.

The small Q_{BD} value of TA-312 is probably caused by irregularities around the SiO_xN_y/Si interface because of inhomogeneity in the film thickness and relatively large undulation have been observed by TEM.

Hydrogen-free nitridation of thin SiO_2 film has been achieved by employing newly developed RTP sequence using only O_2 and N_2O as reactants. The dielectric properties of SiO_2 film can be greatly improved by this process.

H. FUKUDA
T. ARAKAWA
S. OHNO

Semiconductor Technology Laboratory
Oki Electric Industry Co., Ltd
550-5 Higashiasakawa, Hachioji, Tokyo 193, Japan

5th July 1990

References

1 ITO, T., NAKAMURA, T., and ISHIKAWA, H.: 'Advantages of thermal nitride and nitroxide gate films in VLSI process', *IEEE Trans.*, 1982, **ED-29**, pp. 498–502
2 MOSLEHI, M. M., SARASWAT, K. C., and SHATAS, S. C.: 'Rapid thermal nitridation of SiO_2 for nitroxide thin dielectrics', *Appl. Phys. Lett.*, 1985, **47**, pp. 113–1115
3 LAI, S. K., LEE, J., and DHAM, V. K.: 'Electrical properties of nitrided-oxide systems for use in gate dielectrics and EEPROM'. IEEE IEDM Tech. Dig., 1983, pp. 190–193
4 HORI, T., IWASAKI, H., and TSUJI, K.: 'Electrical and physical properties of ultrathin reoxidized nitrided oxides prepared by rapid thermal processing', *IEEE Trans.*, 1989, **36**, pp. 340–349
5 FUKUDA, H., ARAKAWA, T., and OHNO, S.: 'Highly reliable ultra-thin SiO_2 films formed by rapid thermal processing'. IEEE IEDM Tech. Dig., 1989, pp. 451–454
6 WITHAM, H. S., and LENAHAN, P. M.: 'Nature of the E' deep hole trap in metal-oxide-semiconductor oxides', *Appl. Phys. Lett.*, 1987, **51**, pp. 1007–1009

AlGaAs/GaAs SURFACE EMITTING LASER DIODE WITH CURVED REFLECTOR

Indexing term: Semiconductor lasers

An AlGaAs/GaAs surface-emitting laser diode using one step liquid phase epitaxial growth has been successfully fabricated. A micro-cleavage technique was developed to fabricate the mirrors of the laser cavity. The laser beam emitted horizontally from the edge of the laser cavity is converted to the vertical direction using a nearby slant metal reflector formed by pregrowth selective etching of the substrate and subsequent liquid phase epitaxial growth. The maximum power output is beyond 10 mW and the threshold current density achieved is 8 kA/cm². The full width at half maximum of the far field pattern perpendicular to the laser bar is 9°.

Surface-emitting laser diodes are of great interest for their potential applications in wide varieties of fields, e.g., they can be easily integrated into a two dimensional array[1–3] to perform optical parallel processing. When they are used in optoelectronic integrated circuits (OEIC)[4] they provide the possibility to perform wafer to wafer communication.[3] In addition, during the fabrication processes, they do not require a cleavage process to make an optical cavity, and the initial probe test could be performed before their separation into chips and thus reduce the cost of handling and testing. Several types of surface-emitting AlGaAs/GaAs and InGaAsP/InP laser diodes have been demonstrated. Among them, the AlGaAs surface emitting diodes are attractive because they can be applied to optical discs and optical sensing. According to the diode structure and the light propagation path, there are four approaches to achieve surface-emitting laser diodes, i.e., vertical resonator cavity,[5,6] second order grating,[7] 45° mirrors,[8] and parabolic mirrors.[9] In the AlGaAs/GaAs material system, only the first three approaches have been reported. We demonstrate the successful fabrication of a surface emitting laser diode with curved reflectors. Fig. 1 shows all the fabrication steps. The first step is to form a reflector through two selective etchings of the substrate and subsequent liquid phase epitaxy (LPE). The reflector pattern is defined on the substrate surface by the first mask, and the substrate is placed into an etching solution $1H_2SO_4:8H_2O_2:1H_2O$ for 2 min to etch a depth about 1.5 μm into the substrate. The second mask is used to define the active and reflector regions and the substrate is placed again into the etching solution $1H_2SO_4:8H_2O_2:1H_2O$ for 2 min to etch another 1.5 μm in depth. The five layer structure was grown on the etched Zn-doped GaAs substrate by LPE; (1) A 1 μm thick $Al_{0.8}Ga_{0.2}As$ layer Mg-doped to about 1×10^{19} cm^{-3}. The purpose of this layer is to provide a buffer layer which can be overetched by HF + H_2O to form an overhanging structure. (2) A 1 μm thick $Al_{0.36}Ga_{0.64}As$ cladding layer Ge-doped to about 1×10^{18} cm^{-3}. (3) A 1·5 μm thick $Al_{0.05}Ga_{0.95}As$ active layer Ge-doped to about 1×10^{17} cm^{-3}. (4) A 1 μm thick $Al_{0.36}Ga_{0.64}As$ cladding layer Te-doped to about 2×10^{18} cm^{-3}. (5) A 1·2 μm thick $Al_{0.05}Ga_{0.95}As$ cap layer with Te-doped to about 1×10^{19} cm^{-3}.

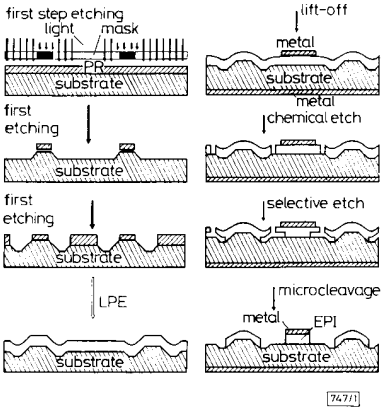

Fig. 1 *Process steps for fabricating surface emitting diode*

Fig. 2*a* shows the photograph of the cross section of the structure after LPE growth. The curved reflector is clearly formed. After the laser cavity was defined by chemical etching

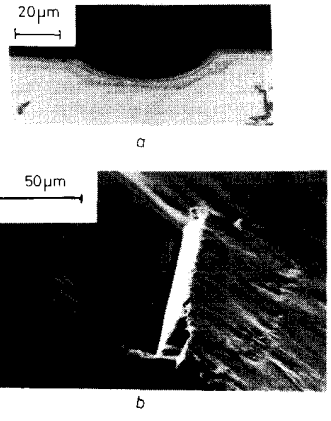

Fig. 2 *Device photographs*
a Cross section of epitaxy profile
b Micro cleaved mirror

and lateral isolation, the metal was evaporated on the laser bar and lifted-off to form an ohmic contact. By using this metal contact as a mask all the epilayers in the exposed area were etched down to the substrate. $HF + H_2O$ was then used to overetch the underlying $Al_{0.8}Ga_{0.2}As$ layer to form an overhanging structure. The laser cavity mirrors were formed by using ultrasonic vibration to break this overhanging structure. Fig. 2*b* shows the micro-cleaved mirror[10] of the laser cavity. Clearly, the mirror was flat and in the [110] natural cleavage plane. Fig. 3 shows the finished device. The laser beam emitted horizontally from the edge will be reflected by the reflector and turn to vertical direction. The shape of the mirror, as shown in Fig. 3, is close to parabolic. Fig. 4 shows the near field pattern of the surface emitting laser diode. The picture was taken from above the surface. The laser beam clearly comes out vertically from the surface. The light against input current (*L–I*) curve are shown in Fig. 5*a*. The threshold

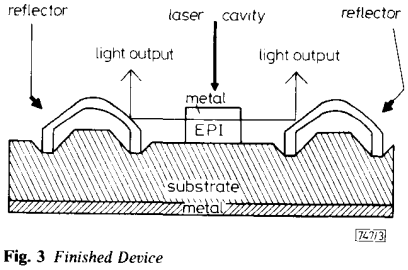

Fig. 3 *Finished Device*
The laser beam emitted horizontally from the edge turns to upward direction by the reflector

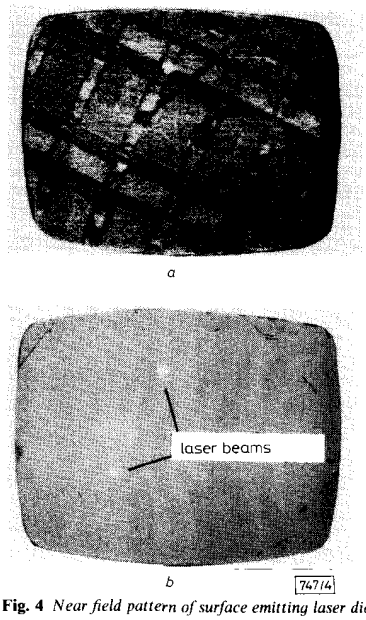

Fig. 4 *Near field pattern of surface emitting laser diode*

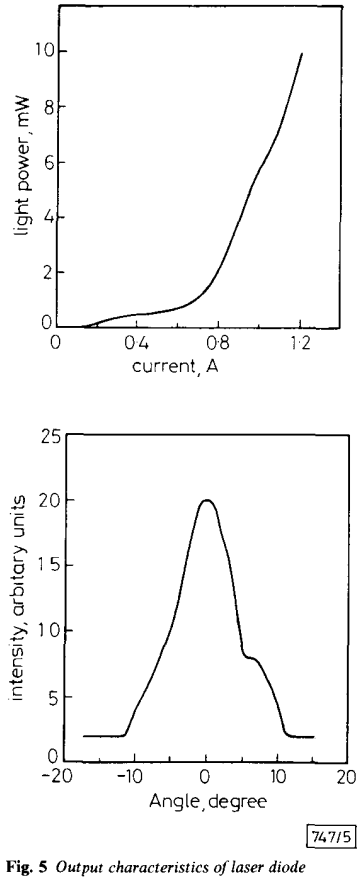

Fig. 5 *Output characteristics of laser diode*
a Light against input current
b Far-field pattern parallel to laser bar

current is 0·7 A which corresponds to a current density of 8 kA/cm^2. The relatively high threshold current is because of the thick (1·5 μm) active layer. The power achieved is 10 mW at an injection current of 1 A. Fig. 5*b* shows the far field pattern parallel to the laser bar measured from above the surface. The full width at half maximum (FWHM) is only 9° at the current of 1 A. It may be caused by the converging effect of the curved reflector.

In conclusion, an AlGaAs/GaAs surface emitting diode with curve reflector has been successfully fabricated. The curved reflector is formed by two pregrowth etching steps and subsequent LPE growth. The diode exhibits high output power of more than 10 mW and narrow far field pattern. These characteristics make it suitable for use in optical discs.

S.-J. YIH
S.-C. LEE
Department of Electrical Engineering
National Taiwan University
Taipei, Taiwan, Republic of China

10th July 1990

References

1 OGURA, M., MUKAI, S., SHIMADA, M., ASAKA, T., YAMASAKI, Y., SEKI, T., and IWANO, H.: 'Surface-emitting laser diode with distributed Bragg reflector and buried heterostructure', *Electron. Lett.*, 1990, **26**, pp. 18–19

2 EVANS, G. A., CARSON, N. W., HAMMER, J. M., LURIE, M., BUTLER, J. K., and PALFREY, S. L.: 'Two-dimensional coherent laser arrays using grating surface emission', *IEEE J. Quantum Electron.*, 1989, **QE-25**, pp. 1525–1536

3 MISSAGGIA, L. J., WALPOLE, J. N., LIAU, Z. L., and PHILLIPS, R. J.: 'Microchannel heat sinks for two-dimensional high-power-density diode', *IEEE J. Quantum Electron.*, 1989, **QE-25**, pp. 1988–1992

4 NODA, S., KOJIMA, K., MITSUNAGA, K., KYUMA, K., HAMANAKA, K., and NAKAYAMA, T.: 'Monolithic integration of an AlGaAs/GaAs multiple quantum well distributed feedback laser and a grating coupler for surface emission', *Appl. Phys. Lett.*, 1987, **51**, pp. 1200–1202

5 OGURA, M., and MUKAI, S.: 'Distributed-feedback surface-emitting laser diode with lateral double heterostructure', *Electron. Lett.*, 1987, **23**, pp. 758–760

6 JEWELL, J. L., MCCALL, S. L., LEE, Y. H., SCHERER, A., GOSSARD, A. C., and ENGLISH, J. H.: 'Lasing characteristics of GaAs microresonators', *Appl. Phys. Lett.*, 1989, **54**, pp. 1400–1402

7 EVANS, G. A., CARLSON, N. W., HAMMER, J. M., LURIE, M., BUTLER, J. K., and CARR, L. A.: 'Efficient, high-power grating surface emitting lasers', *Appl. Phys. Lett.*, 1988, **52**, pp. 1037–1039

8 YANG, J. J., JANSEN, M., and SERGANT, M.: 'Surface-emitting GaAlAs/GaAs laser with etched mirrors', *Electron. Lett.*, 1986, **22**, pp. 438–439

9 LIAU, Z. L., and WALPOLE, J. N.: 'Surface-emitting GaInAsP/InP laser with low threshold current and high efficiency', *Appl. Phys. Lett.*, 1985, **46**, pp. 115–117

10 BLAUVELT, H., CHAIM, N. B., FEKETE, D., MARGALIT, S., and YARIV, A.: 'AlGaAs lasers with microcleaved mirrors suitable for monolithic integration', *Appl. Phys. Lett.*, 1982, **40**, pp. 289–291

STABILITY OF SECOND ORDER TIME-VARYING CONSTRAINED NOTCH FILTERS

Indexing terms: filters, Stability

The stability of second order time-varying constrained notch filters (TVCNF) which are capable of rejecting a sine signal with time-varying frequency is analysed. Two cases are considered: $TVCNF_1$, where one of the two coefficients of the filter is allowed to vary with time while the value of the second coefficient is kept constant; $TVCNF_2$, where both the coefficients can vary with time. It is shown that $TVCNF_2$ is always asymptotically stable while the $TVCNF_1$ possesses unstable regions. Thus for tracking a sine signal with time-varying frequency, $TVCNF_2$ is preferable to $TVCNF_1$.

Introduction: The processing of a multitone signal (enhancement/rejection), is usually carried out by a $2N$ order constrained notch filter (CNF), where N is the number of sinewave components. An adaptive version of such a filter (CANF), has been proposed by Rao and Kung.[1] This filter has been modified by Nehorai,[2] who developed a CNF with N parameters and a variable debiasing coefficient. Those two articles deal with a multitone signal whose parameters, including frequencies, are supposed to be unknown, but with fixed values over the observation interval. As a result, the coefficients of the CANF become functions of the signal frequencies, remaining almost fixed over the steady-state range.

Our interest is in analysing the properties, mainly the stability, of a CNF in the more realistic case where the frequencies of the multitone components vary with time, i.e., where the input signal consists of a sum of frequency modulated (FM) tones. Changes in the frequencies of the signal components cause the parameters of the CNF (being functions of frequencies) to become function of time even in the steady-state range. Such a filter has to be considered as a time-varying CNF (TVCNF), since its coefficients are time-controlled to provide effective tracking of the input signal frequencies.

Our interest is to study the stability properties of a TVCNF; therefore we assume that the rules of frequency variations are known and the time-controlled coefficients of the TVCNF can consequently be calculated prior to the filtering process. Referring to the CANF, such an assumption means that, by using an adaptive procedure, almost ideal tracking of the multitone is achieved. In what follows we also concentrate on a second order TVCNF used for rejection of only one FM component, but the results obtained may be easily extended to a multiple FM signal by exploiting a number of second order sections in cascade connection.

The difference equation of one second order section of TVCNF can be expressed as

$$y(k) + \alpha a_1(k)y(k-1) + \alpha^2 a_2(k)y(k-2) = x(k) + a_1(k)x(k-1) + a_2(k)x(k-2) \quad (1)$$

where α is the debiasing coefficient.[1,2] It is assumed that $0 < \alpha < 1$ which ensures stability of the filter for the time-invariant case.

Let us denote a TVCNF with only one time-controlled coefficient by $TVCNF_1$, a filter with two controlled coefficients is denoted by $TVCNF_2$. Thus in $TVCNF_1$ only $a_1(k)$ is allowed to vary with time and $a_2(k) = 1$; in $TVCNF_2$ $a_1(k)$ as well as $a_2(k)$ are permitted to vary with time.

Filter with one controlled coefficient—$TVCNF_1$: By generalisation of the time-invariant case for which $a_1 = -2\cos\omega_0$, where ω_0 is the frequency of the rejected sinusoidal signal,[2] we choose $a_1(k) = -2\cos\omega(k)$, where $\omega(k)$ denotes the instantaneous frequency of the rejected FM signal. Under the assumption that the sampling rate, $1/\Delta f$, is large enough compared with the maximal frequency of $y(k)$, the discrete case represented by the difference eqn. 1, can be approximated by a continuous one, described by the differential equation

$$\frac{d^2y}{dt^2} + 2\sigma\frac{dy}{dt} + \omega^2(t)y = \frac{d^2x}{dt^2} + \omega^2(t)x \quad (2)$$

where $\omega(t)$ is the continuous version of $\omega(k)$ and σ is a damping coefficient which can be found from the relationship: $\alpha = e^{-\sigma\Delta t}$. Consider the case where α is very close to unity, i.e., the case where $\sigma \approx 0$, and $\omega(t) = \omega_0 + \Delta\omega\cos\Omega t = 2\pi f_0 + 2\pi\Delta f\cos 2\pi Ft$, where $\Delta\omega < \omega_0$ to ensure positive values of the instantaneous frequency $\omega(t)$. We also assume that $\Delta\omega \ll \omega_0$, thus $\omega^2(t) \approx \omega_0^2 + 2\omega_0\Delta\cos\Omega t$. In such a case the homogeneous eqn. 2 will become the well known Mathieu equation[3]

$$\frac{d^2y}{dt^2} + \omega_0\left(1 + \frac{2\Delta\omega}{\omega_0}\cos\Omega t\right)y = 0 \quad (3)$$

It is well known that Mathlieu equation possesses unstable solutions for certain values of the pair $(\Delta\omega, \Omega)$ and for $\omega_0 =$ const.[3] Consequently, the $TVCNF_1$ becomes unstable at least for the case considered above if the frequency of the parameter variation, F, lies in the vicinity of a subharmonic or a harmonic of the natural frequency, f_0, of the system and the

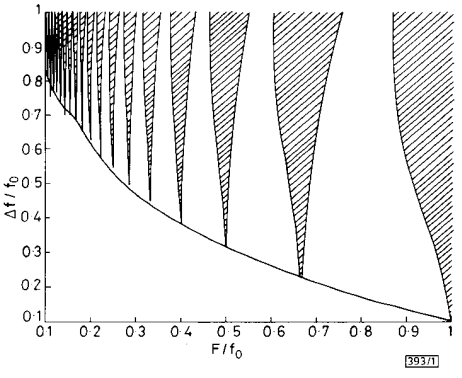

Fig. 1 *Stability diagram for $TVCNF_1$*